Konya Mühendislik Bilimleri Dergisi, c. 12, s. 3, 586-595, 2024
Konya Journal of Engineering Sciences, v. 12, n. 3, 586-595, 2024
ISSN: 2667-8055 (Electronic)
DOI: 10.36306/konjes.1416290

INITIATED CHEMICAL VAPOR DEPOSITION (iCVD) OF POLY(ACRYLIC ACID): A COMPARISON BETWEEN CONTINUOUS AND CLOSED-BATCH iCVD APPROACHES

[1,*] Kurtuluş YILMAZ, [2] Emine SEVGİLİ MERCAN, [3] Mehmet GÜRSOY, [4] Mustafa KARAMAN

Konya Technical University, Engineering and Natural Science Faculty, Chemical Engineering Department, Konya, TÜRKİYE

[1] kurtulusyilmaz3@gmail.com, [2] esmercan@ktun.edu.tr, [3] mgursoy@ktun.edu.tr, [4] mkaraman@ktun.edu.tr

Highlights

- In this study, PAA films were successfully deposited by iCVD method.
- Closed-batch iCVD approach allows the fabrication of more smooth film surface.
- The amount of monomer consumed in the closed batch iCVD method was 18 times less than that of continuous iCVD method.

***Corresponding Author:** Kurtuluş YILMAZ, kurtulusyilmaz3@gmail.com

Konya Mühendislik Bilimleri Dergisi, c. 12, s. 3, 586-595, 2024
Konya Journal of Engineering Sciences, v. 12, n. 3, 586-595, 2024
ISSN: 2667-8055 (Electronic)
DOI: 10.36306/konjes.1416290

INITIATED CHEMICAL VAPOR DEPOSITION (iCVD) OF POLY(ACRYLIC ACID): A COMPARISON BETWEEN CONTINUOUS AND CLOSED-BATCH iCVD APPROACHES

[1,*] Kurtuluş YILMAZ, [2] Emine SEVGİLİ MERCAN, [3] Mehmet GÜRSOY, [4] Mustafa KARAMAN

Konya Technical University, Engineering and Natural Science Faculty, Chemical Engineering Department, Konya, TÜRKİYE

[1] kurtulusyilmaz3@gmail.com, [2] esmercan@ktun.edu.tr, [3] mgursoy@ktun.edu.tr, [4] mkaraman@ktun.edu.tr

(Received: 08.01.2024; Accepted in Revised Form: 10.05.2024)

ABSTRACT: In this study, poly(acrylic acid) (PAA) thin films were deposited on silicon wafer and glass surfaces by initiated chemical vapor deposition (iCVD) method using di-tert-butyl peroxide (TBPO) as the initiator and acrylic acid (AA) as the monomer. During iCVD, two different precursor feeding approaches, namely continuous and closed-batch, were employed. The effects of substrate temperature and the precursor feeding approaches on the deposition rates and surface morphology of the films were investigated. The highest deposition rates for the continuous and closed-batch iCVD approaches were found as 26.1 nm/min and 18.6 nm/min, respectively, at a substrate temperature of 15 °C. FTIR analysis of the films deposited by both approaches indicated high structural retention of the monomer during the polymerization. AFM results indicated that, PAA thin films possessed low RMS roughness values of 2.76 nm and 1.84 nm using continuous and closed-batch iCVD, respectively. Due to the slightly higher surface roughness of the film deposited under continuous iCVD, that film exhibited a lower water contact angle of 16.1° than the film deposited in closed-batch iCVD. In terms of monomer utilization ratio, closed-batch system was found to be more effective, which may help to minimize the carbon footprint of iCVD process.

Keywords: *Poly(acrylic acid), Thin film, Hydrophilic, Chemical vapor deposition, iCVD*

1. INTRODUCTION

Poly(acrylic acid) (PAA), which is obtained by polymerization of acrylic acid monomer and is commercially available in powder form, has a wide range of industrial applications. PAA has a hydrophilic structure that has a high capacity for the retention of water molecules thanks to the carboxyl (-COOH) groups in its structure. Its easy solubility in water, non-toxicity, biodegradability, biocompatibility and excellent optical properties make PAA an important material for various applications such as superabsorbents, adhesives, pharmaceutics, drug delivery, water treatment, personal care products, coatings and packaging [1-5]. Cross-linked PAAs with a more stable structure and superior mechanical properties can be used in applications where linear PAAs cannot be used. For example, linear PAA thin films do not offer a permanent solution for anti-fog applications because they are not resistant to water vapor. However, cross-linked PAA thin films show excellent anti-fog properties [6].

In general, PAA is synthesized commercially in nano/micro particulate, gel, and thin film forms. Thin films of PAA on various surfaces can be formed using two different approaches, namely solvent-based (wet) and vapor-based (dry) processes. Solvent-based methods do not require specialized and expensive equipment, that is why they are widely used. Solvent-based methods for producing PAA homopolymers and copolymers include reversible addition fragmentation chain transfer (RAFT) polymerization [7], atom transfer radical polymerization (ATRP) [8], electrochemically induced free radical polymerization [9], living radical polymerization [10], sol-gel [11], photopolymerization [12] and electrospinning [13]. Nevertheless, there are a number of serious drawbacks to solvent-based techniques, including the need for several time-consuming steps and the possibility of solvent surface damage. In addition, the use of solutions in solvent-based methods can cause environmental and health problems. Environmentally friendly chemical vapor deposition (CVD) technique, as a vapor-based method, eliminate solvent related

***Corresponding Author:** Kurtuluş YILMAZ, kurtulusyilmaz3@gmail.com

problems. CVD offers many advantages such as being a single-step process with short synthesis time, low temperature, substrate independence, adjustable film thickness and scalability [14, 15].

It is possible to produce PAA thin films by two different CVD methods: Plasma enhanced chemical vapor deposition (PECVD) and initiated chemical vapor deposition (iCVD). In PECVD polymerization, the activation energy required to initiate polymerization is provided by plasma discharge. However, high power plasma may lead to the fragmentation of the monomers, which may cause the loss of the functional groups. Furthermore, ion bombardment during PECVD may cause a decrease in the deposition rate [16]. In iCVD process, plasma-induced problems are minimized by the use of heated filaments to initiate the polymerization process. In addition to the monomer, initiator, which has chemical bonds that can be easily radicalized at low temperatures, is fed into the chamber. The presence of initiator ensures the production of polymer thin films with highly functional groups at low temperatures [17].

In this study, iCVD technique was used for the synthesis of PAA thin films. The high-vapor pressure (4 mmHg at 20°C) of acrylic acid (AA) makes it a suitable monomer for iCVD processes. Acrylic acid monomer can be fed into the reactor by evaporation at 23°C ambient temperature, without the need for heating and without the need for a carrier gas. The effect of substrate temperature in PAA synthesis and the effect of continuous or batch chemical feed to the reactor on the deposition rate were investigated. For the first time in literature, a comparison between two monomer feeding approach, namely continuous and closed-batch, were made; and it was shown that closed-batch approach is effective in terms of monomer utilization ratio.

2. MATERIAL AND METHODS

2.1 Materials

Monomer AA (98% purity) and initiator di-tert-butyl peroxide (TBPO) (98% purity) were purchased from Aldrich. The precursors were used without any further purification process. Silicon wafer (University Wafer, 725 μm thickness, ⟨100⟩, p-type and 10–20 Ω·cm) and glass slide (ISOLAB) were used as substrates. The chemical structures of precursors are displayed in Figure 1(a).

2.2 Methods

A schematic diagram of the custom-built iCVD reactor that was used in this study is given in Figure 1(b). A more detailed description of iCVD process is given elsewhere [18]. Substrates were placed on the bottom of the reactor, which was cooled by water from a recirculating chiller (Lab Comp., RW-0525G), with the substrate temperature adjustable between 15 and 30°C. The reactor has a 2.5 cm thick quartz top plate which allows in-situ monitoring of the film thickness using a laser interferometry system. In the interferometry, the intensity of a diode laser (Huanic, DI650-1-5) with a wavelength of 650 nm light from the silicon wafer was measured using a laser power meter (Thorlabs). A vacuum was created in the reactor using a rotary vane vacuum pump (Edwards RV12). The chamber pressure was measured using a capacitive pressure sensor (MKS Baratron) and for all depositions the initial pressure set values were adjusted to be at 600 mTorr. The pressure during deposition was controlled and maintained at the desired level by a PID-controlled butterfly valve (MKS) placed between the reactor and the vacuum pump. The heat energy required to initiate polymerization during iCVD was provided by heating a 12-turn tungsten (Alfa Aesar, 99.9%) filament array that was suspended 2.5 cm above the sample surface to be deposited using a variac (Varsan). The K-type thermocouple (Omega) was used to measure the temperature of a randomly selected wire. The temperature of the filament and reactor wall were both kept constant at 230°C and 36°C, respectively. The AA monomer and TBPO initiator were evaporated at 23°C ambient temperature in two separate stainless-steel vessels and their vapors were introduced into the reactor at ambient temperature via needle valves. Two different precursor feeding approaches were employed during iCVD polymerization. In the first one, the precursors were fed to the reactor and the by-product vapors were pumped-out of the reactor in continuous manner. In the second one, the precursors were fed

to the reactor sequentially until desired pressure was reached and then the reactor in and out valves were all closed [19]. The former way of deposition is named as continuous, and the latter one is named as closed-batch. In continuous system, iCVD films were deposited at an AA flow rate of 0.95 sccm, and a TBPO flow rate of 0.95 sccm with a filament temperature of 230 C. The same filament temperature was used in closed-batch iCVD, also. The experimental details of the iCVD deposition of PAA are summarized in Table 1.

Table 1. iCVD parameters used in the experiments of this study.

Sample name	Precursor flow approach	Substrate temperature (°C)	AA / TBPO ratio	Reactor pressure (mtorr)
PAA1	Continuous	15	1/1	600
PAA2	Continuous	20	1/1	600
PAA3	Continuous	25	1/1	600
PAA4	Continuous	30	1/1	600
PAA5	Closed-batch	15	1/1	600
PAA6	Closed-batch	20	1/1	600
PAA7	Closed-batch	25	1/1	600
PAA8	Closed-batch	30	1/1	600

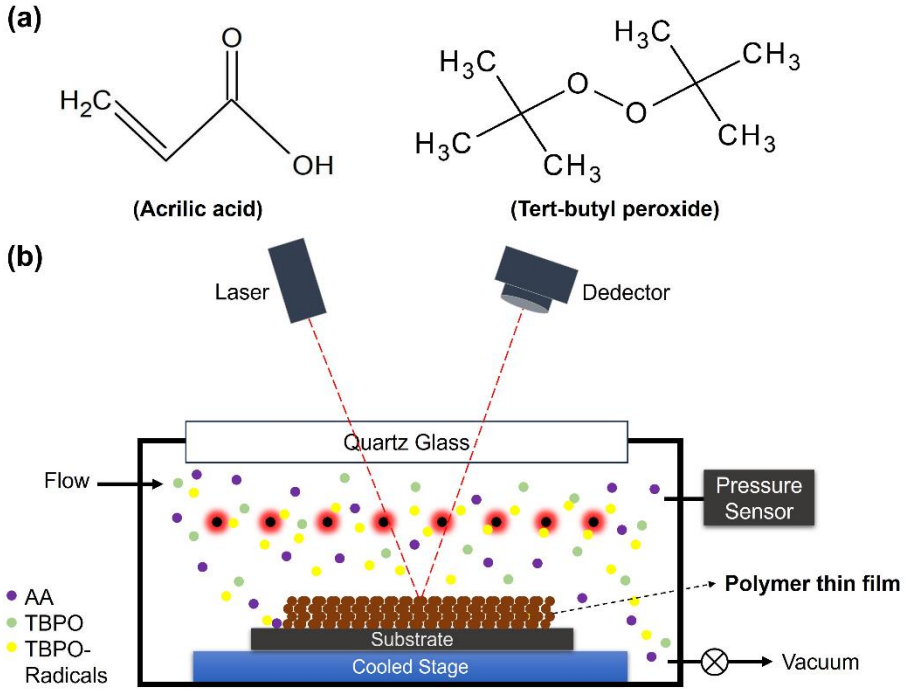

Figure 1. a) Chemical structures of the precursors used in this study, b) schematic diagram of the iCVD reactor

2.3 Characterizations

The chemical structures of the as-deposited PAA thin films were characterized by FTIR spectrophotometer (Thermo Scientific, Nicolet iS 10), which performed a total of 32 scans at 4 cm^{-1} resolution between 400–4000 cm^{-1} wavenumbers. The surface topographies and roughness values of the as-deposited PAA thin films on silicon wafers were analyzed by AFM (NT-MDT) in semi-contact mode with a scanning area of 10 × 10 μm^2. To confirm the interferometric thickness measurements of PAA thin films, an ex-situ film thickness measurement was carried out with a thin film reflectometer (Avantes Avaspec-ULS2048L). Water contact angle analysis was performed of the as-deposited PAA thin films

coated silicon wafer using 4.0 μL of DI water and a video capture system (Kruss Easy Drop). PAA thin film optical transmission spectra were obtained in the 400–800 nm wavelength range using a UV/vis spectrophotometer (Shimadzu UV-1800) with a spectral resolution of 1 nm.

3. RESULTS AND DISCUSSION

The effect of substrate temperature and feeding approaches of precursors into the reactor on the deposition rates at constant pressure and monomer/initiator ratio was investigated and the results are summarized in Figure 2. The reported deposition rates in Figure 2 were obtained by dividing the thickness of as-deposited film on the silicon wafer by the total deposition time. The deposition rates of PAA thin films deposited by the continuous iCVD method were calculated to be 26.1, 20, 15.8 and 12.4 nm/min at substrate temperatures 15, 20, 25 and 30 °C, respectively. The films deposited under closed-batch conditions were deposited at rates of 18.6, 15.3, 10.4 and 8.5 nm/min at substrate temperatures 15, 20, 25 and 30 °C, respectively. The lower deposition rates in closed-batch approach as compared to the continuous approach can be attributed to the decrease in the concentration of the precursor as reactants are consumed with time [19, 20]. In continuous approach, since the precursors are continuously fed to the reactor, constant reactant concentrations are achieved, which in turn keeps the deposition rates constant and high. In that perspective, it can be said that continuous approach is advantageous in terms of the deposition rates. However, in terms of the monomer consumption amount, which we define as the amount of monomer consumed per 100 nm as-deposited film, the closed batch configuration appeared to be more advantageous. In closed-batch approach, only 37.8 mg of AA monomer consumed per 100 nm as-deposited film, whereas in continuous approach the monomer consumption was found as 680 mg for the same amount of film production, which indicated a nearly 18-fold higher monomer consumption in continuous iCVD.

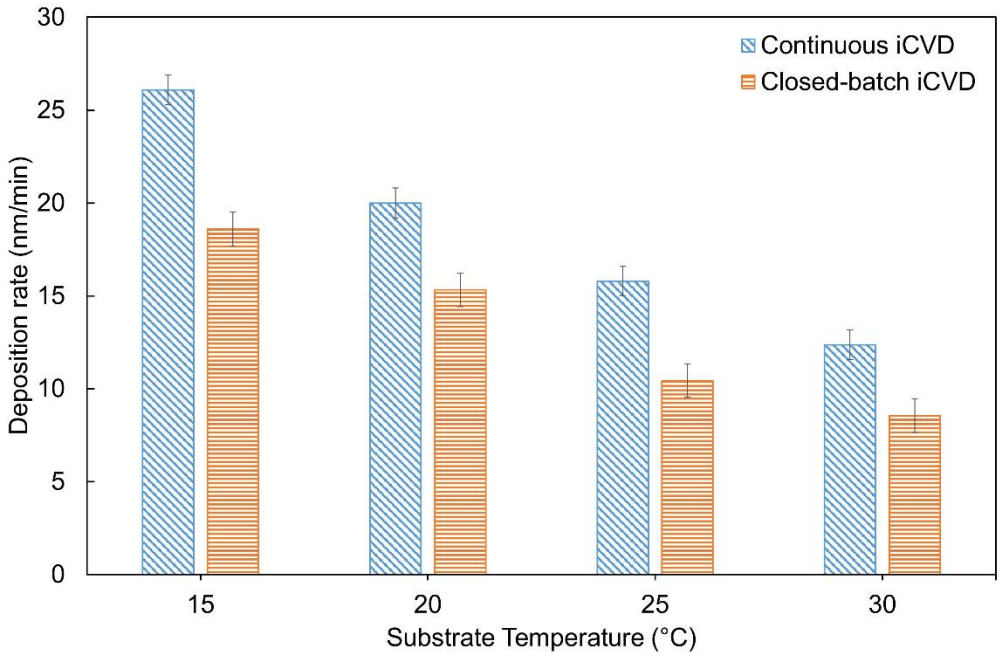

Figure 2. Effect of substrate temperature on deposition rate using continuous and closed-batch iCVD

Activation energies were calculated using Arrhenius equation to investigate the effect of substrate temperature on the deposition rates. Semilogarithmic graphic of the deposition rates on silicon wafer versus different substrate temperatures is given in Figure 3 (a,b). A negative activation energy was observed during PAA thin film depositions in both cases, indicating that PAA deposition is adsorption limited [21-23]. The activation energies of PAA thin films as-deposited by continuous and closed-batch

iCVD approaches were calculated as -35.94 kJ/mol and -39.44 kJ/mol, respectively. The observed small difference in the activation energies can be attributed to the changes in the deposition rates in both cases. In the continuous iCVD approach, the reactant concentration and reaction pressure are constant, whereas in the closed-batch iCVD approach, the reactant concentration and reaction pressure change throughout the polymerization. The reactant concentration decreases during polymerization in the closed-batch iCVD method, which in turn reduces the partial pressure (Pm)/monomer saturation pressure (Psat) value [20, 24]. Pm/Psat is an important parameter in iCVD kinetics that can affect the deposition rate [22, 25]. A decrease in the Pm/Psat ratio can change the activation energy required to initiate polymerization, which in turn can affect the deposition rate [26, 27].

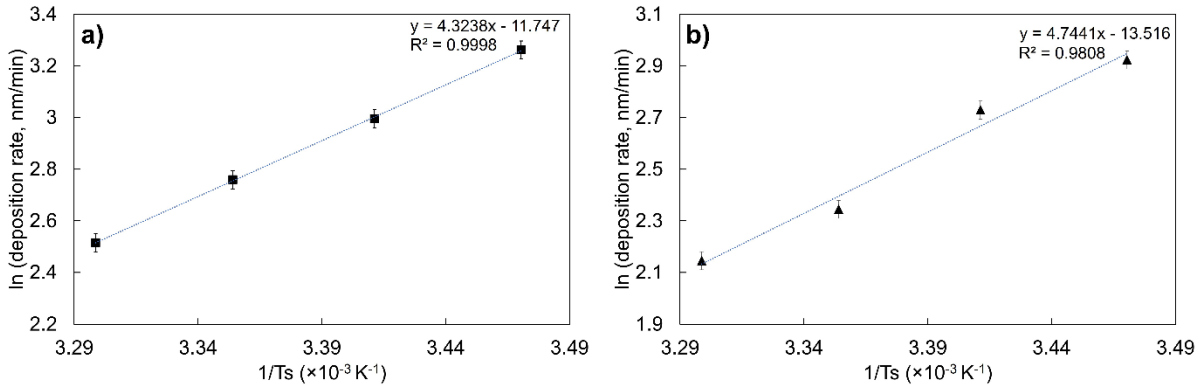

Figure 3. The deposition rate as a function of substrate temperature for PAA activation energy calculation in (a) continuous and (b) closed-batch iCVD process.

The chemical structures of PAA thin films deposited on glass substrate by both iCVD methods was revealed by FTIR analysis. The FTIR spectrum of monomer AA is compared with the spectra of PAA thin films deposited at a substrate temperature of 15°C by both iCVD approaches in Figure 4. The presence of AA is evidenced by broad O-H stretching in the 3671-2169 cm-1 range. The strong absorption peak at 1701 cm^{-1} assigned the carboxyl group (-COOH), which is a clear fingerprint of PAA [6, 28, 29]. The other major vibrational spectra of PAA revealed the C-H stretching, C-H bending, C-O-H bending, C-O stretching and O-H bending vibrations at 2933, 1538, 1440, 1237 and 805 cm^{-1}, respectively [30-33]. The peak at approximately 2351 cm^{-1} corresponds to the CO_2 bond [34]. The increase in the intensity of this peak is thought to indicate that the CO_2 in the atmosphere was not very well stabilized during the measurement. The FTIR analysis revealed a C=C stretching peak at 1634 cm^{-1} in the spectrum of the monomer, but it was not observed in the spectrum of the PAA deposited by the continuous and closed-batch iCVD method. This suggests that the polymerization occurs via an unsaturated C=C bond [35, 36]. According to the FTIR results, it is seen that the carbonyl and hydroxyl groups in the structure of the monomer are well preserved in both PAA thin films [37, 38].

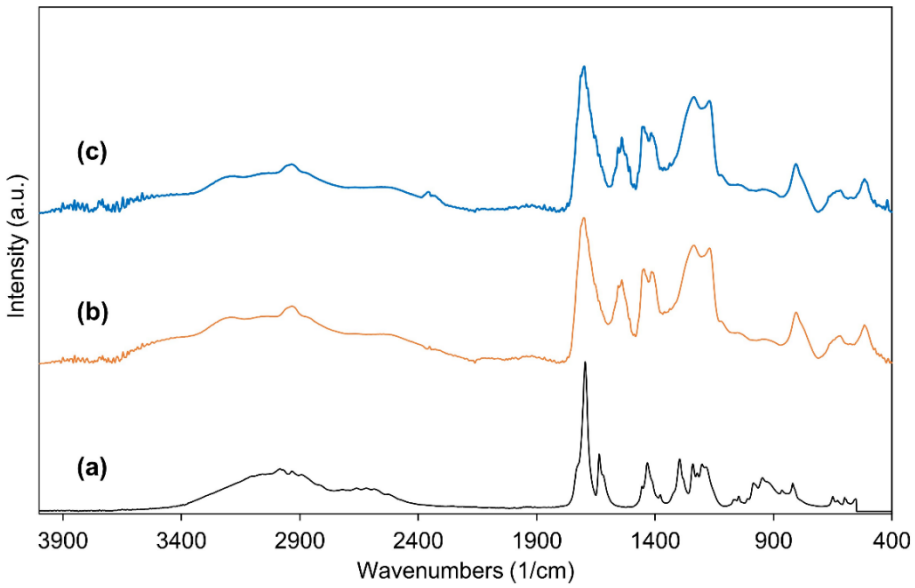

Figure 4. FTIR spectra of (a) AA monomer, PAA thin films deposited by (b) continuous and (c) closed-batch iCVD method.

UV-vis transmittance results of uncoated and PAA coated glasses at 15°C substrate temperature are presented in Figure 5. It can be clearly seen that PAA deposition on the glass slightly reduces the optical transmittance. The 100 nm-thick PAA thin film has a refractive index of 1.527 at wavelength of 633 nm [39, 40]. The refractive index of PAA thin films deposited by iCVD method is higher than the refractive index of glass (n_{glass}=1.5), which slightly reduced the transmittance of glass. The possible reason for the reduced transmittance can also be attributed to the changed surface structure of the PAA thin films [41-43]. The UV-vis spectra of deposited PAA thin films using both iCVD techniques gave similar results in the visible region. All samples showed a very high optical transmittance in the visible region.

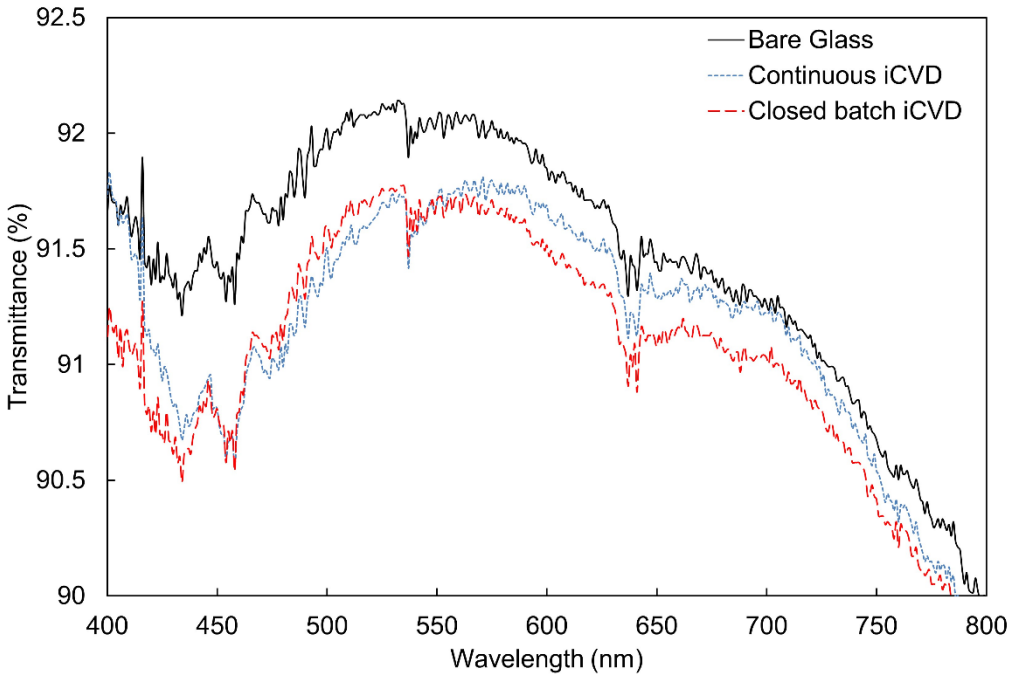

Figure 5. UV-vis spectra of bare and PAA coated glasses at 15°C substrate temperature.

The average roughness (Ra), root mean square (Rq) values and 3D AFM images of PAA films deposited by both iCVD approaches are shown in Figure 6 (a,c). Ra and Rq values of bare silicon wafer were given in our previous study as 0.482 nm and 0.596 nm, respectively [44]. PAA films deposited by the continuous iCVD approach have a rougher surface compared to those deposited by the closed-batch iCVD approach. The lower roughness of films produced by the closed-batch iCVD approach may be a consequence of the slower deposition rate [45]. The water contact angle images are given in Figure 6 (b,d). The water contact angle value of bare silicon wafer was given as 57.6±0.2° in our previous study [44]. The water contact angle values of PAA films deposited by continuous and closed-batch iCVD methods were measured as 16.1 ± 0.06° and 24.4 ± 0.73°, respectively. Wettability of materials depends on surface energy and surface roughness. The increase in surface roughness of materials with high surface energy increases wettability. [46]. This may be the reason why the PAA thin film deposited by continuous iCVD has a lower water contact angle value.

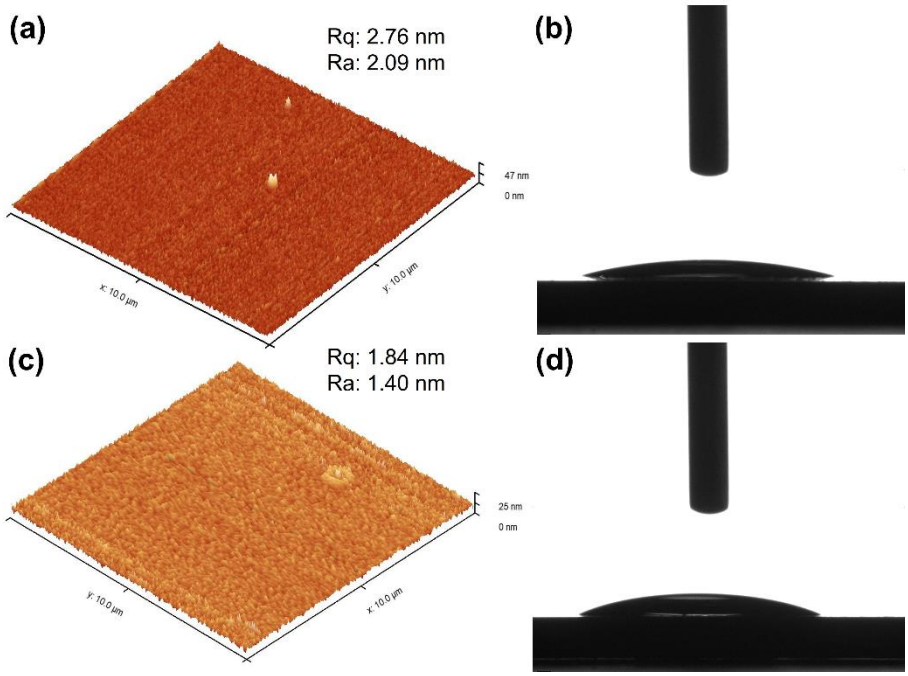

Figure 6. The AFM and water contact angle images of the PAA thin films deposited on silicon wafers by (a,b) continuous and (c,d) closed-batch iCVD at 15°C substrate temperature.

4. CONCLUSIONS

PAA films were successfully deposited by iCVD method on glass and silicon wafer surfaces. In continuous and closed-batch approaches, the highest deposition rates were obtained at a substrate temperature of 15 °C. The apparent activation energies of PAA thin films deposited by continuous and closed-batch iCVD methods were calculated to be -35.94 kJ/mol and -39.44 kJ/mol, respectively. The negative activation energies implied an adsorption-limited iCVD regime. AFM results showed that the closed-batch approach allows the fabrication of more smooth film surface. The amount of monomer consumed to produce a 100-nm-thick film in the closed-batch iCVD approach was 18 times less than that of continuous iCVD approach. Therefore, in terms of monomer utilization ratio, closed-batch system appeared to be more effective, which may help to minimize the carbon footprint of iCVD process.

Declaration of Ethical Standards

The authors declare that the study complies with all applicable laws and regulations and meets ethical standards.

Declaration of Competing Interest

The authors declare that they have no known competing financial interests or personal relationships that could have appeared to influence the work reported in this paper.

Funding / Acknowledgements

The authors thank to Konya Technical University Research Foundation (Project No: 232216033) and the Scientific and Technological Research Council of Turkey (TÜBİTAK, Project No: 118M041) for the financial support of this study.

5. REFERENCES

[1] L. Cui, R. Wang, X. Ji, M. Hu, B. Wang, and J. Liu, "Template-assisted synthesis of biodegradable and pH-responsive polymer capsules via RAFT polymerization for controlled drug release," Materials Chemistry and Physics, vol. 148, no. 1, pp. 87-95, 2014/11/14/ 2014, doi: https://doi.org/10.1016/j.matchemphys.2014.07.016.

[2] H. Arkaban et al., "Polyacrylic acid nanoplatforms: Antimicrobial, tissue engineering, and cancer theranostic applications," Polymers, vol. 14, no. 6, p. 1259, 2022.

[3] A. B. Rashid and M. E. Hoque, "Polymer nanocomposites for defense applications," in Advanced Polymer Nanocomposites: Elsevier, 2022, pp. 373-414.

[4] A. Kausar, "Poly (acrylic acid) nanocomposites: Design of advanced materials," Journal of Plastic Film & Sheeting, vol. 37, no. 4, pp. 409-428, 2021.

[5] Y. Zhao, J. Kang, and T. Tan, "Salt-, pH-and temperature-responsive semi-interpenetrating polymer network hydrogel based on poly (aspartic acid) and poly (acrylic acid)," Polymer, vol. 47, no. 22, pp. 7702-7710, 2006.

[6] K. Yılmaz, M. Gürsoy, and M. Karaman, "Vapor Deposition of Transparent Antifogging Polymeric Nanocoatings," Langmuir, vol. 37, no. 5, pp. 1941-1947, 2021/02/09 2021, doi: 10.1021/acs.langmuir.0c03437.

[7] I. Chaduc, A. Crépet, O. Boyron, B. Charleux, F. D'Agosto, and M. Lansalot, "Effect of the pH on the RAFT polymerization of acrylic acid in water. Application to the synthesis of poly (acrylic acid)-stabilized polystyrene particles by RAFT emulsion polymerization," Macromolecules, vol. 46, no. 15, pp. 6013-6023, 2013.

[8] A. Pal, D. Das, A. K. Sarkar, S. Ghorai, R. Das, and S. Pal, "Synthesis of glycogen and poly (acrylic acid)-based graft copolymers via ATRP and its application for selective removal of Pb2+ ions from aqueous solution," European Polymer Journal, vol. 66, pp. 33-46, 2015.

[9] K. Shi, Y. Lei, S. Wang, and K. K. Shiu, "Electrochemically Induced Free-Radical Polymerization for the Fabrication of Amperometric Glucose Biosensors," Electroanalysis, vol. 22, no. 20, pp. 2366-2375, 2010.

[10] C. Burguière et al., "Block copolymers of poly (styrene) and poly (acrylic acid) of various molar masses, topologies, and compositions prepared via controlled/living radical polymerization. Application as stabilizers in emulsion polymerization," Macromolecules, vol. 34, no. 13, pp. 4439-4450, 2001.

[11] F. Zhang, W. Zhang, Y. Yu, B. Deng, J. Li, and J. Jin, "Sol–gel preparation of PAA-g-PVDF/TiO2 nanocomposite hollow fiber membranes with extremely high water flux and improved antifouling property," Journal of Membrane Science, vol. 432, pp. 25-32, 2013.

[12] B. Yang, Y. Zhou, W. Yu, S. Zhang, H. Chen, and J. Ye, "Photopolymerization synthesis of polyacrylic acid dispersant with methoxysilicon end groups and its application in a nano-SiO2 aqueous system," Polymer International, vol. 68, no. 4, pp. 675-683, 2019.

[13] J. Xie et al., "Phosphate functionalized poly (vinyl alcohol)/poly (acrylic acid)(PVA/PAA): an electrospinning nanofiber for uranium separation," Journal of Radioanalytical and Nuclear

Chemistry, vol. 326, no. 1, pp. 475-486, 2020.
[14] M. Gürsoy and M. Karaman, "Surface Treatments for Biological, Chemical, and Physical Applications," Wiley Online Library, 2016.
[15] K. K. Gleason, "CVD Polymers: Fabrication of Organic Surfaces and Devices," Wiley, p. 8, 2015.
[16] J. Xu and K. K. Gleason, "Conformal, amine-functionalized thin films by initiated chemical vapor deposition (iCVD) for hydrolytically stable microfluidic devices," Chemistry of Materials, vol. 22, no. 5, pp. 1732-1738, 2010.
[17] K. K. Gleason, "Organic surface functionalization by initiated CVD (iCVD)," Surface modification of polymers: methods and applications, pp. 107-134, 2019.
[18] M. Gürsoy et al., "Bioinspired fog capture and channel mechanism based on the arid climate plant Salsola crassa," Colloids and surfaces a: physicochemical and engineering aspects, vol. 529, pp. 195-202, 2017.
[19] K. Yılmaz, H. Şakalak, M. Gürsoy, and M. Karaman, "Vapor deposition of stable copolymer thin films in a batch iCVD reactor," Journal of Applied Polymer Science, 2020, doi: 10.1002/app.50119.
[20] C. D. Petruczok, N. Chen, and K. K. Gleason, "Closed batch initiated chemical vapor deposition of ultrathin, functional, and conformal polymer films," Langmuir, vol. 30, no. 16, pp. 4830-7, Apr 29 2014, doi: 10.1021/la500543d.
[21] M. Gürsoy and M. Karaman, "Effect of substrate temperature on initiated plasma enhanced chemical vapor deposition of PHEMA thin films," physica status solidi (c), vol. 12, no. 7, pp. 1006-1010, 2015.
[22] K. K. Lau and K. K. Gleason, "Initiated chemical vapor deposition (iCVD) of poly (alkyl acrylates): A kinetic model," Macromolecules, vol. 39, no. 10, pp. 3695-3703, 2006.
[23] M. Gürsoy, "Vapor deposition polymerization of synthetic rubber thin film in a plasma enhanced chemical vapor deposition reactor," Journal of Applied Polymer Science, vol. 138, no. 4, p. 49722, 2021.
[24] K. Yılmaz, H. Şakalak, M. Gürsoy, and M. Karaman, "Initiated Chemical Vapor Deposition of Poly(Ethylhexyl Acrylate) Films in a Large-Scale Batch Reactor," Industrial & Engineering Chemistry Research, vol. 58, no. 32, pp. 14795-14801, 2019/08/14 2019, doi: 10.1021/acs.iecr.9b02213.
[25] K. K. Lau and K. K. Gleason, "Initiated chemical vapor deposition (iCVD) of poly (alkyl acrylates): an experimental study," Macromolecules, vol. 39, no. 10, pp. 3688-3694, 2006.
[26] A. Khlyustova and R. Yang, "Initiated Chemical Vapor Deposition Kinetics of Poly (4-Aminostyrene)," Frontiers in Bioengineering and Biotechnology, p. 309, 2021.
[27] M. E. Alf et al., "Chemical vapor deposition of conformal, functional, and responsive polymer films," Advanced Materials, vol. 22, no. 18, pp. 1993-2027, 2010.
[28] J. Wu, Z. Feng, C. Dong, P. Zhu, J. Qiu, and L. Zhu, "Synthesis of sodium carboxymethyl cellulose/poly (acrylic acid) microgels via visible-light-triggered polymerization as a self-sedimentary cationic basic dye adsorbent," Langmuir, vol. 38, no. 12, pp. 3711-3719, 2022.
[29] L. M. Sanchez, D. G. Actis, J. S. Gonzalez, P. M. Zélis, and V. A. Alvarez, "Effect of PAA-coated magnetic nanoparticles on the performance of PVA-based hydrogels developed to be used as environmental remediation devices," Journal of Nanoparticle Research, vol. 21, pp. 1-16, 2019.
[30] T. Kavitha, I.-K. Kang, and S.-Y. Park, "Poly (acrylic acid)-grafted graphene oxide as an intracellular protein carrier," Langmuir, vol. 30, no. 1, pp. 402-409, 2014.
[31] V. d. A. M. Gonzaga, B. A. Chrisostomo, A. L. Poli, and C. C. Schmitt, "Preparation, characterization and photostability of nanocomposite films based on poly (acrylic acid) and montmorillonite," Materials Research, vol. 21, 2018.
[32] D. Lin-Vien, N. B. Colthup, W. G. Fateley, and J. G. Grasselli, The handbook of infrared and Raman characteristic frequencies of organic molecules. Elsevier, 1991.
[33] P. K. Kashyap, Y. S. Negi, N. K. Goel, R. K. Diwan, and S. Rattan, "Chemical initiator-free synthesis of poly (acrylic acid-co-itaconic acid) using radiation-induced polymerization for application in

dental cements," Radiation Physics and Chemistry, vol. 198, p. 110243, 2022.
[34] J. Huang, F. Carpentier, F. Miserque, M. Ferry, and S. Esnouf, "Interaction between radio-oxidized polypropylene and gaseous HCl. Part 1. Qualitative evidence," Polymer Degradation and Stability, vol. 221, p. 110663, 2024/03/01/ 2024, doi: https://doi.org/10.1016/j.polymdegradstab.2024.110663.
[35] W. E. Tenhaeff and K. K. Gleason, "Initiated and oxidative chemical vapor deposition of polymeric thin films: iCVD and oCVD," Advanced Functional Materials, vol. 18, no. 7, pp. 979-992, 2008.
[36] M. Karaman et al., "Chemical and Physical Modification of Surfaces," in Surface Treatments for Biological, Chemical, and Physical Applications, 2017, pp. 23-66.
[37] K. K. Gleason, "Nanoscale control by chemically vapour-deposited polymers," Nature Reviews Physics, vol. 2, no. 7, pp. 347-364, 2020/07/01 2020, doi: 10.1038/s42254-020-0192-6.
[38] K. K. Gleason, "Designing organic and hybrid surfaces and devices with initiated chemical vapor deposition (iCVD)," Advanced Materials, p. 2306665, 2023.
[39] F. Jabeen, M. Chen, B. Rasulev, M. Ossowski, and P. Boudjouk, "Refractive indices of diverse data set of polymers: A computational QSPR based study," Computational Materials Science, vol. 137, pp. 215-224, 2017, doi: 10.1016/j.commatsci.2017.05.022.
[40] L.-Q. Chu, W.-J. Tan, H.-Q. Mao, and W. Knoll, "Characterization of UV-induced graft polymerization of poly (acrylic acid) using optical waveguide spectroscopy," Macromolecules, vol. 39, no. 25, pp. 8742-8746, 2006.
[41] B. Liu, L. Wen, and X. Zhao, "The surface change of TiO2 film induced by UV illumination and the effects on UV–vis transmission spectra," Applied Surface Science, vol. 255, no. 5, pp. 2752-2758, 2008.
[42] M. Eita, L. Wågberg, and M. Muhammed, "Thin films of zinc oxide nanoparticles and poly (acrylic acid) fabricated by the layer-by-layer technique: A facile platform for outstanding properties," The Journal of Physical Chemistry C, vol. 116, no. 7, pp. 4621-4627, 2012.
[43] S. Walheim, E. Schaffer, J. Mlynek, and U. Steiner, "Nanophase-separated polymer films as high-performance antireflection coatings," Science, vol. 283, no. 5401, pp. 520-522, 1999.
[44] M. Gürsoy and B. Kocadayıoğulları, "Environmentally Friendly Approach for the Plasma Surface Modification of Fabrics for Improved Fog Harvesting Performance," Fibers and Polymers, vol. 24, no. 10, pp. 3557-3567, 2023.
[45] S. M. Rumrill, V. Agarwal, and K. K. S. Lau, "Conformal Growth of Ultrathin Hydrophilic Coatings on Hydrophobic Surfaces Using Initiated Chemical Vapor Deposition," Langmuir, vol. 37, no. 25, pp. 7751-7759, Jun 29 2021, doi: 10.1021/acs.langmuir.1c00918.
[46] K.-Y. Law, "Contact Angle Hysteresis on Smooth/Flat and Rough Surfaces. Interpretation, Mechanism, and Origin," Accounts of Materials Research, vol. 3, no. 1, pp. 1-7, 2022/01/28 2022, doi: 10.1021/accountsmr.1c00051.